

# Generalized logistic growth modeling of the COVID-19 outbreak in 29 provinces in China and in the rest of the world

Ke Wu<sup>1,2</sup>, Didier Darcet<sup>3</sup>, Qian Wang<sup>2,4</sup> and Didier Sornette<sup>1,2\*</sup>

<sup>1</sup> *Institute of Risk Analysis, Prediction and Management (Risks-X), Academy for Advanced Interdisciplinary Studies, Southern University of Science and Technology (SUSTech), Shenzhen, China*

<sup>2</sup> *Chair of Entrepreneurial Risks, Department of Management, Technology and Economics (D-MTEC), ETH Zurich, Zurich, Switzerland*

<sup>3</sup> *Gavekal Intelligence Software, Nice, France*

<sup>4</sup> *Department of Banking and Finance, University of Zurich, Zurich, Switzerland*

\* Corresponding author, [dsornette@ethz.ch](mailto:dsornette@ethz.ch)

**Acknowledgements:** We benefitted from many stimulating discussions and exchanges with Michael Schatz, Peter Cauwels, Dmitry Chernov, Euan Mearns, Pengcheng Li and Yixuan Zhang.

## Abstract

The COVID-19 has been successfully contained in China but is spreading all over the world. We calibrate the logistic growth model, the generalized logistic growth model, the generalized Richards model and the generalized growth model to the reported number of infected cases from for the whole of China, 29 provinces in China, and 19 countries and regions that are undergoing major outbreaks. We dissect the development of the epidemics in China and the impact of the drastic control measures both at the aggregate level and within each province. We quantitatively document four phases of the outbreak in China with a detailed analysis on the heterogeneous situations across provinces. The extreme containment measures implemented by China were very effective with some instructive variations across provinces. Borrowing from the experience of China, we made scenario projections on the development of the outbreak in other countries. We identified that Europe and US have passed the inflection point and entered into an after-peak trajectory, which is estimated longer than what a classical Logistic model predicts, in contrast to most provinces in China where the after-peak trajectory is much faster. We expect Europe to have 1.83 million final total confirmed cases (2452 per million population) and US to have 1.26 million final total confirmed cases (3851 per million population). We identified three groups of countries in different level of outbreak progress, and provide informative implications for the current global pandemic.

## Keywords

*Novel coronavirus (COVID-19), logistic growing, epidemic modeling, prediction*

## 1. Introduction

Starting from Hubei province in China, the novel coronavirus (SARS-CoV-2) has been spreading all over the world after two months of outbreak in China. Facing uncertainty and irresolution in December 2019 and the first half of January 2020, China then responded efficiently and massively to this new disease outbreak by implementing unprecedent containment measures to the whole country, including lockdown the whole province of Hubei and putting most of other provinces in de-facto quarantine mode. Since March 2020, one and a half month after the national battle against the COVID-19 epidemic, China has managed to contain the virus transmission within the country, with new daily confirmed cases in mainland China excluding Hubei in the single digit range, and with just double digit numbers in Hubei. In contrast, many other countries have had fast increasing numbers of confirmed cases since March 2020, which leads to a resurgence in China due to the imported cases from overseas. On March 11, the World Health Organization (WHO) declared the coronavirus outbreak as a global pandemic. As of April 25, there are more than 2.8 million cases are confirmed in more than 185 countries and territories, with 1.8 million active cases and close to 200 thousand deaths.

For an epidemic to develop, three key ingredients are necessary: 1) Source: pathogens and their reservoirs; 2) Susceptible persons with a way for the virus to enter the body; 3) Transmission: a path or mechanism by which viruses moved to other susceptible persons. Numerous mechanistic models based on the classical SIR model and its extensions have been utilized to study the COVID-19 epidemic. Within such a multi-agent framework, one can detail different attributes among countries, including the demographics, climate, population density, health care systems, government interference, etc., which will affect the three key ingredients of the epidemic mentioned above. There is a large amount of literature using this framework studying the past major epidemics [1-6] as well as the current COVID-19 outbreak in different regions and countries[7-11]. Notably, a report from Neil Ferguson at Imperial College London [12] using such a framework projected future scenarios with different government strategies have made a large impact on the government policies.

Although mechanistic models are useful in understanding the effect of different factors on the transmission process, they are highly sensitive to the assumptions on the many often subtle microscopic processes. Giving an illusion of precision, mechanistic models are in general quite

fragile and require an in-depth understanding of the dominating processes, which are likely to be missing in the middle and confusion of the pandemics, with often inconsistent and unreliable statistics and studies performed under strong time pressure. There is thus space for simpler and, we argue, more robust phenomenological models, which have low complexity but enjoy robustness. This is the power of coarse-graining, a well-known robust strategy to model complex system [13-15].

In this paper, we focus on using phenomenological models without detailed microscopic foundations, but which have the advantage of allowing simple calibrations to the empirical reported data and providing transparent interpretations. Phenomenological approaches for modeling disease spread are particularly suitable when significant uncertainty clouds the epidemiology of an infectious disease, including the potential contribution of multiple transmission pathways [16]. In these situations, phenomenological models provide a starting point for generating early estimates of the transmission potential and generating short-term forecasts of epidemic trajectory and predictions of the final epidemic size [16].

There have been quite an extensive literature reporting statistical analysis and future scenarios of COVID-19 epidemic based on phenomenological models. Many of previous work use simple exponential growth models and focus on the early growing process [17-21]. On the other hand, there are also many works arguing that the number of infected people follows a trajectory different from a simple exponential growth [22-26].

In this paper, we employ the classical Logistic growth model, the Generalized Logistic Model (GLM), the Generalized Richards Model and the Generalized Growth Model (GGM), which have been successfully applied to describe previous epidemics [16,27-30]. All these models have some limitations and are only applicable in some stages of the outbreak, or when enough data points are available to allow for sufficiently stable calibration. For example, an epidemic follows an exponential or quasi-exponential growth at an early stage (following the law of proportional growth), so the Generalized Growth Model is more suitable here. Then, the growth rate decays as fewer susceptible people are available for infection and countermeasures are introduced to hinder the transmission of the virus, so the Logistic type of models are better in this later stage.

In this paper, we explain the data and the models in details in section 2 and 3. In section 4 and 5, we calibrate different models to the reported number of infected cases in the COVID-19 epidemics from Jan. 19 to March 10 for the whole of China and 29 provinces in mainland China.

Then in Section 6, we perform a similar modeling exercise on other countries that are undergoing major outbreaks of this virus.

Our analysis dissects the development of the epidemics in China and the impact of the drastic control measures both at the aggregate level and within each province. Borrowing from the experience of China, we made projections on the development of the outbreak in other countries. Our study employs simple models to quantitatively document the effects of the Chinese containment measures against the SARS-CoV-2 virus, and provide informative implications for the current global pandemic.

## 2. Data

**Confirmed cases:** we focus on the daily data of confirmed cases. For data from mainland China, the data source is national and provincial health commission. We exclude the epicenter province, Hubei, which had a significant issue of underreporting at the early stage and also data inconsistency during mid-Feb due to a change of classification guidelines. For the provinces other than Hubei, the data is consistent except for one special event on Feb 20 concerning the data coming from several prisons.

We do not include the Chinese domestic data after March 10 because we conclude that the major outbreak between Jan and March was contained and finished. Although there have been resurgences of cases after mid-March due to imported cases from overseas countries, it is another transmission dynamics compared with the Jan-Mar major outbreak, and the risk of another round of epidemic is low given the continuing containment measures and massive testing programs [31].

For data in other countries, the source is European Centre for Disease Prevention and Control (ECDC) [32], which updated every day at 1pm CET, reflecting data collected up to 6:00 and 10:00 CET. Note that the cases of the Diamond Princess cruise are excluded from Japan, following the WHO standard.

**Data adjustment:** On Feb 20, for the first time, infected cases in the Chinese prison system were reported, including 271 cases from Hubei, 207 cases from Shandong, 34 cases from Zhejiang. These cases were concealed before because the prison system was not within the coverage of each provincial health commission system. Given that the prison system is relatively independent and the cases are limited, We remove these cases in our data for the modelling analysis to ensure consistency.

**Migration data:** the population travels from Hubei and Wuhan to other provinces from Jan 1<sup>st</sup> to Jan 23<sup>rd</sup> are retrieved from the Baidu Migration Map (<http://qianxi.baidu.com>).

### 3. Method

At an early stage of the outbreak, an exponential or generalized exponential model can be used to describe the data, which is intuitive and easy to calibrate. This has been employed to describe the initial processes of the epidemic in many cases, including influenza, Ebola, foot-and-mouth disease, HIV/AIDS, plague, measles, smallpox [28] and also COVID-19 [21]. A Generalized Growth model (GGM) is defined as:

$$\frac{dC(t)}{dt} = rC^p(t), \quad (1)$$

where  $C(t)$  represents the cumulative number of confirmed cases at time  $t$ ,  $p \in [0,1]$  is an exponent that allows the model to capture different growth profiles including the constant incidence ( $p = 0$ ), sub-exponential growth ( $0 < p < 1$ ) and exponential growth ( $p = 1$ ). In the latter case, the solution is  $C(t) = C_0 e^{rt}$ , where  $r$  is the growth rate and  $C_0$  is the initial number of confirmed cases at the time when the count starts. For  $0 < p < 1$ , the solution of equation (1) is  $C(t) = C_0 \left(1 + \frac{rt}{A}\right)^b$ , where  $b = \frac{1}{1-p}$  and  $A = \frac{C_0^{1-p}}{1-p}$ , so that  $r$  controls the characteristic time scale of the dynamics. Essentially, the (quasi) exponential model provides an upper bound for future scenarios by assuming that the outbreak continues to grow following the same process as in the past.

However, an outbreak will slow down and reach its limit with decaying transmission rate in the end, resulting in the growth pattern departing from the (sub-)exponential path as the cumulative number of cases approaches its inflection point and the daily incidence curve approaches its maximum. Then, a Logistic type model could have a better performance. In fact, the exponential model and the classical Logistic model are the first- and second-order approximations to the growth phase of an epidemic curve produced by the standard Kermack–McKendrick SIR model [33,34]. To account for different subtle dynamics in different stages of an epidemic, we use three types of Logistic models when the outbreak is leaving the early growth stage:

- Classical Logistic growing model:

$$\frac{dC(t)}{dt} = rC(t) \left(1 - \frac{C(t)}{K}\right) \quad (2)$$

- Generalized Logistic model (GLM):

$$\frac{dC(t)}{dt} = rC^p(t) \left(1 - \frac{C(t)}{K}\right) \quad (3)$$

- Generalized Richards model (GRM):

$$\frac{dC(t)}{dt} = r[C(t)]^p \left(1 - \left(\frac{C(t)}{K}\right)^\alpha\right) \quad (4)$$

These three models all include two common parameters: a generalised growth rate  $r$  setting the typical time scale of the epidemic growth process and the final capacity  $K$ , which is the asymptotic total number of infections over the whole epidemics. In the Generalized Logistic model, one additional parameter  $p \in [0,1]$  is introduced on top of the classical Logistic model to capture different growth profiles, similar to the generalized growth model (1). In the Generalized Richards model, the exponent  $\alpha$  is introduced to measure the deviation from the symmetric S-shaped dynamics of the simple logistic curve. The GRM recovers the original Richards model [35] for  $p = 1$ , and reduces to the classical logistic model (2) for  $\alpha = 1$  and  $p = 1$ . Therefore, the GRM is more pertinent when calibrating data from a region that has entered the after-peak stage, to better describe the after-peak trajectory that may have deviated from the classical Logistic decay due for instance to various containment measures. However, this more flexible model leads to more unstable calibrations if used on early stage data.

For the calibrations performed here, we use the standard Levenberg–Marquardt algorithm to solve the non-linear least square optimization for the incidence curve. For the fitting of the classical logistic growth function, we free the initial point  $C_0$  and allow it to be one of the 3 parameters  $(C_0, K, r)$  to be calibrated, as the early stage growth does not follow a logistic growth. However, for the fitting of the remaining three models,  $C_0$  is fixed at the empirical value. To estimate the uncertainty of our model estimates, we use a bootstrap approach with a negative binomial error structure  $\text{NB}(\mu, \sigma^2)$ , where  $\mu$  and  $\sigma^2$  are the mean and variance of the distribution, estimated from the empirical data.

In the next section, we apply the most flexible model, the Generalized Richards Model (GRM), to study the 29 provinces in China where the outbreak is at the end. The GRM has four free parameters and is able to characterize the different epidemic patterns that developed in the 29 provinces. We also fit the classical Logistic model to the daily incidence data as a comparison with

the GRM, and a simple exponential decay model to the growth rate of cumulative confirmed cases to provide another perspective.

In Section 5, we apply the four models (Eq. 1-4) to various countries and regions to identify their epidemic progress and potential future scenarios. Logistic type models tend to under-estimate the final capacity  $K$  and thus could serve as lower bounds of the future scenarios [36,37]. The classical Logistic model is the least flexible one among the three and usually provides the lowest estimate of the final capacity, because it fails to account for 1) the sup-exponential growth which could be captured by the GLM; 2) the potential slow abating of the epidemic which could be captured by the GRM. Both factors will increase the estimated final total confirmed numbers and they both require more data to calibrate. The performance of more flexible models increases as more data (especially data after the inflection point of the cumulative number) becomes available for calibration. Given the above, we define three scenarios that can be described by these four models. The **positive scenario** is defined by the model with the second lowest predicted final total confirmed cases  $K$  among the three Logistic models, and the **medium scenario** is described by the model with the highest predicted final total deaths among the three Logistic models. It is important to note that both positive and medium scenarios could underestimate largely the final capacity, especially at the early stage of the epidemics. The **negative scenario** is described by the Generalized Growth model, which should only describe the early stage of the epidemic outbreak and is therefore least reliable for countries in the more mature stage as it does not include a finite population capacity.

## 4. Analysis at the global and provincial level for China (excluding Hubei)

### 4.1 Analysis at the aggregate level of mainland China (excluding Hubei)

As of March 10<sup>th</sup>, 2020, there were in total 13172 infected cases reported in the 30 provinces in mainland China outside Hubei. The initially impressive rising statistics have given place to a tapering associated with the limited capacity for transmission, exogenous control measure, and so on. In Figure 1, the trajectory of the total confirmed cases, the daily increase of confirmed cases, and the daily growth rate of confirmed cases in whole China excluding Hubei province are

presented. The fits with the generalized Richards model and with the classical logistic growth model are shown in red and blue lines respectively in the upper, middle and lower left panel, with the data up to March 1<sup>st</sup>, 2020. In the lower left panel of Figure 1, the daily empirical growth rate  $r(t) := \log \frac{C(t)}{C(t-1)}$  of the confirmed cases is plotted in log scale against time. We can observe two exponential decay regimes of the growth rate with two different decay parameters before and after Feb-14, 2020. The green line is the fitted linear regression line (of the logarithm of the growth rate as a function of time) for the data from Jan-25 to Feb 14, 2020, yielding an exponential decay parameter equal to -0.157 per day (95% CI: (-0.164, -0.150)). This indicates that, after the lockdown of Wuhan city on Jan 23 and the top-level health emergency activated in most provinces on Jan 25, the transmission in provinces outside Hubei has been contained with a relatively fast exponential decay of the growth rate from a value starting at more than 100% to around 2% on Feb 14. Then, starting Feb 15, three weeks after a series of extreme controlling measures, the growth rate is found to decay with a faster rate with a decay parameter equal to -0.277 per day (95% CI: (-0.313, -0.241)).

This second regime is plotted as the cyan line in the lower left panel of Figure 1. The green and cyan straight lines show the linear regression of the logarithm of the growth rate as a function of time for the period of Jan 25 to Feb 14, and the period of Feb 15 to Mar 1, respectively. The asymptotic exponential decay of the growth rate can be justified theoretically from the generalized Richards model (4) by expanding it in the neighborhood where  $C$  converges to  $K$ . Introducing the change of variable  $C(t) = K(1 - \varepsilon(t))$ , and keeping all terms up to first order in  $\varepsilon(t)$ , equation (4) yields

$$\frac{d\varepsilon(t)}{dt} = -\gamma\varepsilon(t) \quad \text{with} \quad \gamma = r\alpha K^{p-1}. \quad (5)$$

This gives

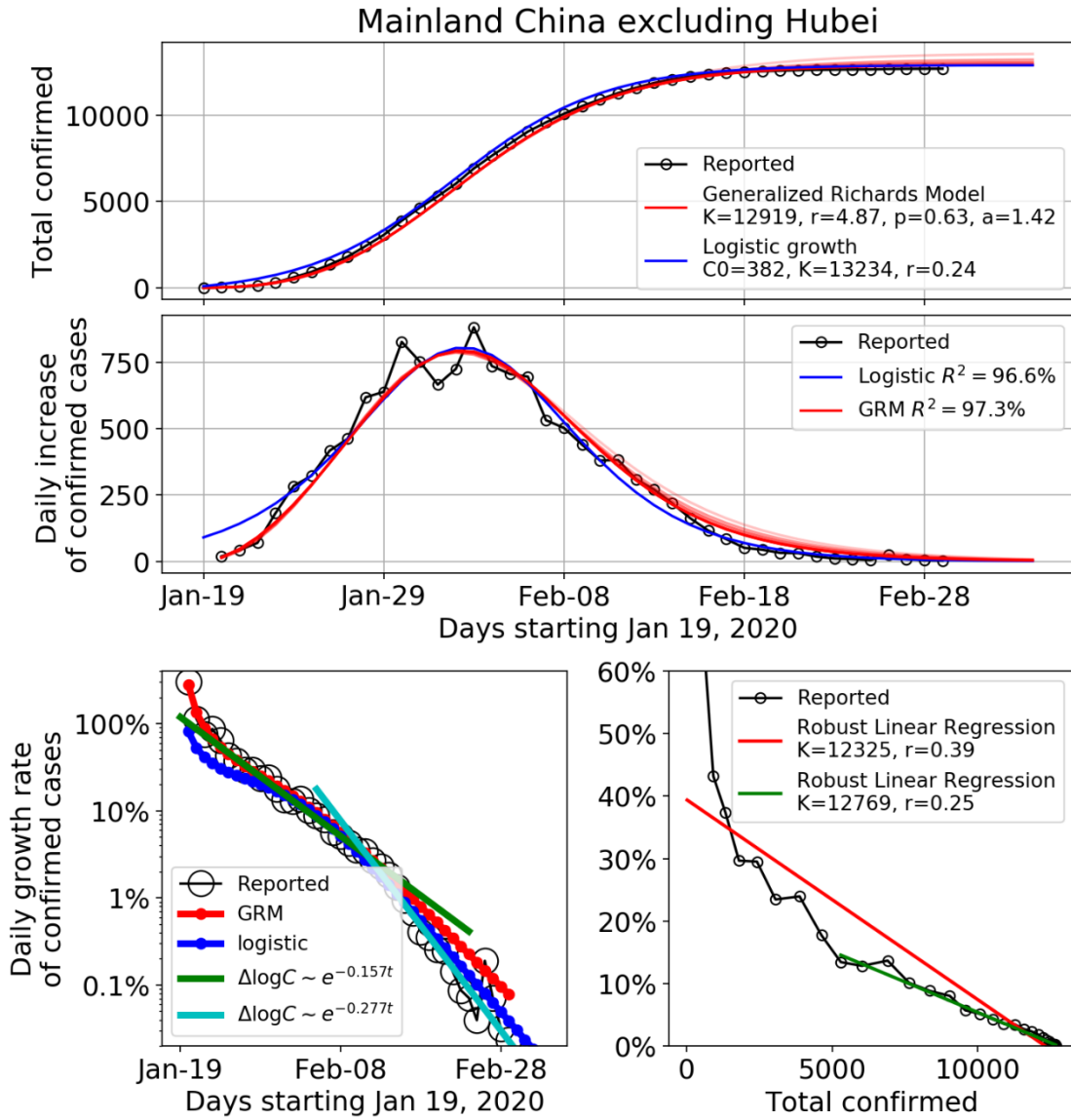
$$\frac{1}{C} \frac{dC(t)}{dt} = \frac{\epsilon_0 \gamma e^{-\gamma t}}{1 - \epsilon_0 e^{-\gamma t}} = \gamma (\epsilon_0 e^{-\gamma t} + [\epsilon_0 e^{-\gamma t}]^2 + [\epsilon_0 e^{-\gamma t}]^3 + \dots), \quad (6)$$

where  $\varepsilon_0$  is a constant of integration determined from matching this asymptotic solution with the non-asymptotic dynamics far from the asymptote. Thus, the leading behavior of the growth rate at long times is  $\frac{1}{C} \frac{dC(t)}{dt} = \gamma \epsilon_0 e^{-\gamma t}$ , which is exponential decaying as shown in the lower left panel of Figure 1. Using expression (5) for  $\gamma$  as a function of the 4 parameters  $r, \alpha, K$  and  $p$  given in

the inset of the top panel of Figure 1, we get  $\gamma = 0.21$  for mainland China excluding Hubei, which is bracketed by the two fitted values 0.17 and 0.28 of the exponential decay given in the inset of the lower left panel of Figure 1.

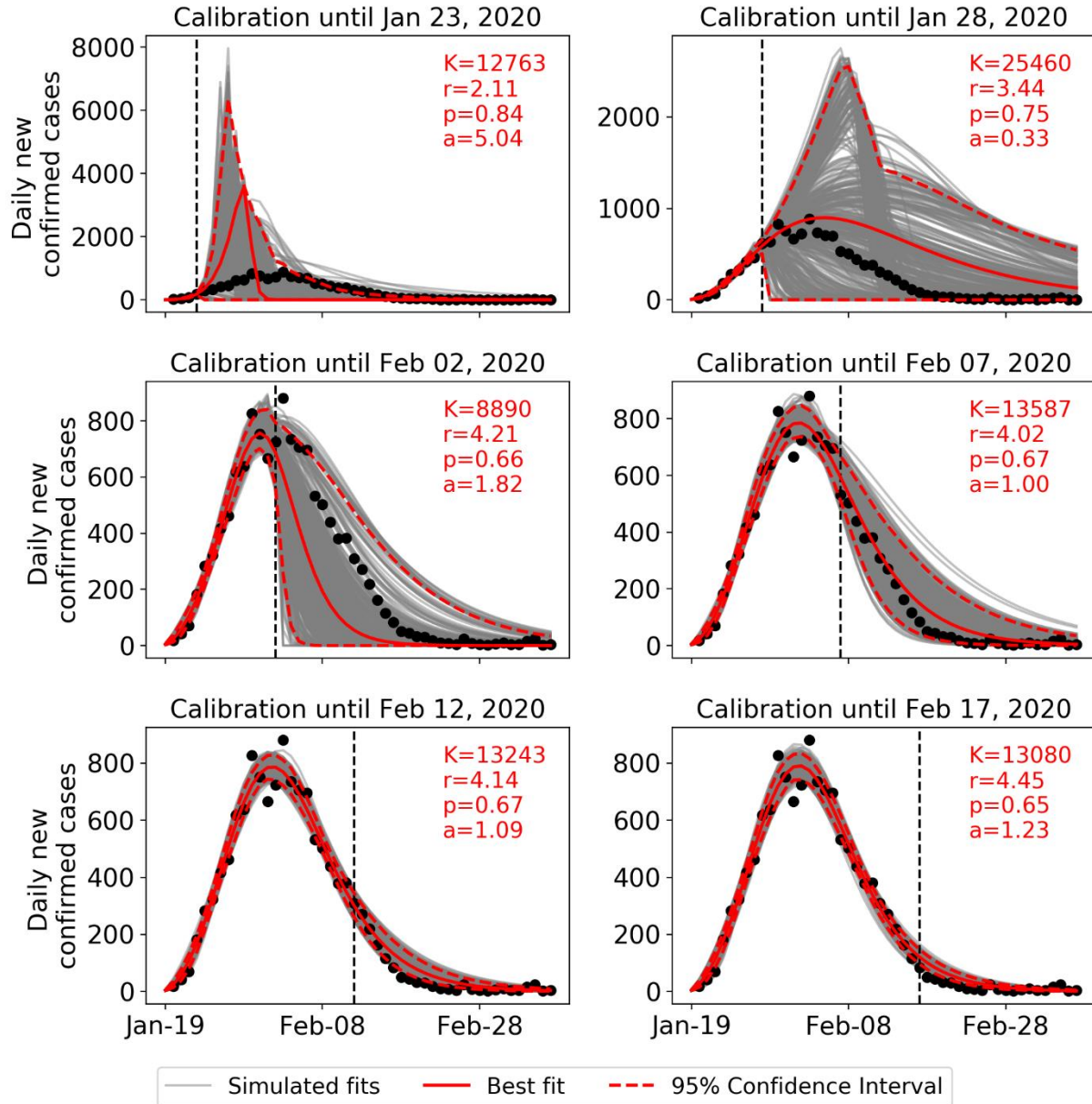
In the lower right panel of Figure 1, the empirical growth rate  $r(t)$  is plotted in linear scale against the cumulative number of confirmed cases. The red and green lines are the linear regressed lines for the full period and for the period after Feb 1<sup>st</sup>, 2020 respectively. We can see that the standard logistic growth cannot capture the full trajectory until Feb 1<sup>st</sup>. After Feb 1<sup>st</sup>, the linear fit is good, qualifying the simple logistic equation ( $p = 1$  and  $\alpha = 1$ ), with growth rate  $r$  estimated as 0.25 for the slope, which is compatible with the value determined from the calibration over the full data set shown in the top two panels of Figure 1.

Figure 2 demonstrates the sensitivity of the calibration of the GRM to the end date of the data by presenting six sets of results for six end dates. Specifically, the data on the daily number of new confirmed case is assumed to be available until 23 Jan, 28 Jan, 2 Feb, 7 Feb, 12 Feb, 17 Feb, i.e. 30, 25, 20, 15, 10 and 5 days before Feb 22 were presented. For each of the six data sets, we generated 500 simulations of  $\frac{dC(t)}{dt}$  based on the best fit parameters using parametric bootstrap with a negative binomial error structure, as in prior studies [28]. Each of these 500 simulations constitutes a plausible scenario for the daily number of new confirmed cases, which is compatible with the data and GRM. The dispersion among these 500 scenarios provides a measure of stability of the fits and their range of values gives an estimation of the confidence intervals. The first conclusion is the non-surprising large range of scenarios obtained when using data before the inflection point, which however encompass the realized data. We observe a tendency for early scenarios to predict a much faster and larger number of new cases than observed, which could be expected in the absence of strong containment control. With more data, the scenarios become more accurate, especially when using realized data after the peak, and probably account now well for the impact of the containment measures that modified the dynamics of the epidemic spreading.



**Figure 1.** Time dependence of the total number of confirmed cases (upper panel), the daily number of new confirmed cases (middle panel), and the daily growth rate of confirmed cases (lower panel) in the mainland China excluding Hubei province until March 1<sup>st</sup>, 2020. The empirical data is marked by the empty circles. The blue and red lines in the upper, middle and lower left panels show the fits with the Logistic Growth Model and Generalized Richards Model (GRM) respectively. For the GRM, we also show the fits using data ending 20, 15, 10, 5 days earlier than March 1<sup>st</sup>, 2020, as lighter red lines in the upper and middle panel. This demonstrates the consistency and robustness of the fits. The lower left panel shows the daily growth rate of the confirmed cases in log scale against time. The green and cyan straight lines show the linear regression of the logarithm of the growth rate as a function of time for the period of Jan 25 to Feb 14, and the period of Feb 15 to Mar 1, respectively. The lower right panel is the daily growth rate of the confirmed cases in linear scale against the cumulative number of confirmed

cases. The red and green lines are the linear fits for the period of Jan 19 to Feb 1, and the period of Feb 2 to Mar 1, respectively.



**Figure 2.** Daily number of new observed confirmed cases for mainland China excluding Hubei (black circles) compared with 500 scenarios built by parametric bootstrap with a negative binomial error structure on the GRM model with best fit parameters determined on the data up to the time indicated by the vertical dashed line. The last time used in the calibration is respectively 5, 10, 15, 20, 25, 30 days before Feb 22, 2020 from bottom to top. The red continuous line is the best fitted line and the two dashed red curves delineate the 95% confidence interval extracted from the 500

scenarios. The six panels correspond each to a different end date, shown as the sub-title of each panel, at which the data has been calibrated with the GRM model.

## **4.2 Analysis at the provincial level (29 provinces) of mainland China (excluding Hubei)**

As of March 1, 2020, the daily increase of the number of confirmed cases in China excluding Hubei province has decreased to less than 10 cases per day. The preceding one-month extreme quarantine measures thus seems to have been very effective from an aggregate perspective, although there is a resurgence of cases since mid-March due to imported cases from overseas countries. At this time, it is worthwhile to take a closer look at the provincial level to study the effectiveness of measures in each province. The supplementary material presents figures similar to Figure 1 for each of the 29 provinces in mainland China. Tibet is excluded as it only has 1 confirmed case as of March 10. Table 1 provides some useful statistics for each province and the values of the fitted parameters of the generalized Richards model, logistic growth model and the exponential decay exponent of the growth rate. This analysis at the 29 provinces allows us to identify four phases in the development of the epidemic outbreak in mainland China.

**Table 1:** Summary statistics for 29 provinces in mainland China (excluding Hubei and Tibet), as of Feb 29, 2020. The values of the fitted parameters of the generalized Richards model, logistic growth model and the exponential decay exponent are reported.

	Cumulative number of cases	Population density (2018, per km <sup>2</sup> )	Population (2018, million)	Date of 1st reported case	Generalized Richards Model					Logistic Growth Model				Exponential decay of the growth rate			# of days between 1st reported date and the peak of daily
					K	r	p	a	R-squared	K	C <sub>0</sub>	r	R-squared	a	95% Confidence Interval	R-squared	
Guangdong	1352	481	111.7	19-Jan-20	1322	1.00	0.84	0.74	90.7%	1344	24.3	0.29	91.1%	-0.159	(-0.139, -0.179)	92.7%	13
Henan	1272	553	95.6	21-Jan-20	1266	2.42	0.61	1.88	74.4%	1302	37.6	0.28	75.0%	-0.186	(-0.161, -0.210)	92.8%	11
Zhejiang	1242	460	56.6	20-Jan-20	1190	1.30	1.00	0.19	82.3%	1220	37.0	0.31	80.8%	-0.223	(-0.201, -0.244)	95.0%	10
Hunan	1018	304	68.6	21-Jan-20	1043	2.94	0.56	1.68	91.8%	1084	50.9	0.25	91.4%	-0.166	(-0.154, -0.178)	97.4%	12
Anhui	990	429	62.5	20-Jan-20	987	3.78	0.47	3.48	91.8%	1045	24.0	0.25	92.1%	-0.167	(-0.149, -0.186)	90.4%	15
Shandong	960	579	100.1	20-Jan-20	553	3.69	0.39	4.83	69.8%	604	27.2	0.22	67.6%	-0.163	(-0.138, -0.189)	90.4%	17
Jiangxi	935	247	46.2	20-Jan-20	966	0.99	0.82	0.75	89.0%	980	19.8	0.27	88.4%	-0.173	(-0.156, -0.190)	94.8%	15
Jiangsu	631	742	80.3	22-Jan-20	655	3.40	0.45	2.45	93.6%	697	43.9	0.22	93.0%	-0.149	(-0.139, -0.158)	97.4%	10
Chongqing	576	374	30.5	21-Jan-20	584	3.90	0.41	2.18	80.6%	633	61.7	0.20	80.5%	-0.142	(-0.121, -0.163)	90.0%	11
Sichuan	539	172	83.0	20-Jan-20	564	11.73	0.87	0.02	87.0%	597	51.8	0.18	82.7%	-0.145	(-0.130, -0.159)	94.9%	11
Heilongjiang	481	81	37.9	21-Jan-20	481	0.63	1.00	0.34	73.9%	494	7.9	0.26	73.7%	-0.118	(-0.091, -0.145)	67.6%	14
Beijing	426	1323	21.7	20-Jan-20	401	0.98	0.68	1.49	77.8%	413	19.4	0.23	78.4%	-0.156	(-0.122, -0.189)	84.1%	11
Shanghai	342	3814	24.2	20-Jan-20	330	1.49	0.59	1.88	86.7%	345	14.0	0.26	88.1%	-0.160	(-0.138, -0.182)	87.9%	11
Hebei	318	355	75.2	22-Jan-20	310	3.16	0.31	11.82	72.0%	350	22.2	0.19	65.4%	-0.130	(-0.099, -0.161)	79.9%	16
Fujian	296	285	39.1	22-Jan-20	302	39.51	0.91	0.01	91.0%	315	27.9	0.26	85.8%	-0.200	(-0.180, -0.220)	95.2%	7
Guangxi	252	190	48.9	20-Jan-20	251	4.64	0.22	3.92	68.4%	292	28.1	0.18	68.5%	-0.144	(-0.102, -0.186)	76.2%	11
Shaanxi	245	185	38.4	22-Jan-20	249	1.11	0.68	1.02	70.0%	258	20.4	0.24	70.0%	-0.171	(-0.140, -0.201)	87.4%	10
Yunnan	174	109	48.0	20-Jan-20	169	11.86	1.00	0.02	63.7%	161	6.2	0.33	57.2%	-0.195	(-0.146, -0.245)	75.5%	9
Hainan	168	224	9.3	20-Jan-20	168	2.49	0.27	8.07	65.2%	189	11.9	0.19	60.1%	-0.084	(-0.038, -0.129)	49.2%	16
Guizhou	146	200	35.8	20-Jan-20	150	0.66	0.61	8.39	75.0%	156	1.7	0.27	72.1%	-0.150	(-0.112, -0.188)	78.5%	20
Tianjin	136	1306	15.6	21-Jan-20	138	0.86	0.53	2.62	45.2%	146	8.4	0.19	45.4%	-0.111	(-0.057, -0.164)	44.7%	14
Shanxi	133	212	37.0	21-Jan-20	130	1.72	0.38	7.44	84.9%	142	5.8	0.26	83.2%	-0.193	(-0.170, -0.217)	91.7%	13
Liaoning	125	291	43.7	22-Jan-20	124	2.02	0.35	2.92	62.0%	137	15.3	0.22	62.0%	-0.132	(-0.091, -0.173)	74.1%	7
Jilin	119	151	27.2	20-Jan-20	87	2.18	0.22	25.81	66.0%	103	10.3	0.23	63.1%	-0.187	(-0.139, -0.236)	78.0%	14
Gansu	93	57	26.3	23-Jan-20	87	0.32	1.00	1.41	72.8%	83	0.1	0.44	74.6%	-0.158	(-0.117, -0.199)	77.4%	9
Xinjiang	76	13	24.4	23-Jan-20	78	0.92	0.38	11.42	68.7%	83	4.3	0.20	60.1%	-0.087	(-0.063, -0.110)	59.7%	18
Neimenggu/Inner Mongolia	75	20	25.3	23-Jan-20	77	1.56	0.28	2.94	50.9%	88	11.7	0.18	51.2%	-0.135	(-0.092, -0.179)	67.9%	11
Ningxia	75	85	6.8	20-Jan-20	71	1.27	0.27	88.28	55.7%	84	6.2	0.17	41.3%	-0.102	(-0.049, -0.155)	50.6%	22
Qinghai	18	7	6.0	24-Jan-20	18	1.20	0.13	100.00	50.9%	24	4.0	0.27	39.7%	-0.227	(-0.092, -0.362)	71.0%	8
China exclude Hubei	13213	141	1325.7	19-Jan-20	12919	4.87	0.63	1.42	97.3%	13234	382.8	0.24	96.6%	-0.157	(-0.164, -0.150)	99.2%	14

- **Phase I (Jan 19 – Jan 24, 6 days): early stage outbreak.** The data mainly reflects the situation before Jan 20, when no measures were implemented, or they were of limited scope. On Jan 19, Guangdong became the first province to declare a confirmed case outside Hubei in mainland China [22]. On Jan 20, with the speech of President Xi, all provinces started to react. As of Jan 24, 28 provinces reported confirmed cases with daily growth rates of confirmed cases ranging from 50% to more than 100%.
- **Phase II (Jan 25 – Feb 1, 8 days): fast growth phase approaching the peak of the incidence curve (inflection point of the cumulative number).** The data starts to reflect the measures implemented in the later days of Phase I and in Phase II. In this phase, the government measures against the outbreak have been escalated, marked by the lockdown of Wuhan on Jan 23, the top-level public health emergency state declared by 20+ provinces by Jan 25, and the standing committee meeting on Jan 25, the first day of the Chinese New Year, organized by President Xi, to deploy the forces for the battle against the virus outbreak. In this phase, the growth rate of the number of confirmed cases in all provinces are declining from 50% to 10%+, with an exponentially decay rate of 0.157 for the aggregated data. At the provincial level, some provinces failed to see a continuous decrease of the growth rate and witnessed the incidence grow at a constant rate for a few days, implying exponential growth of the confirmed cases. These provinces include Jiangxi (~40% until Jan 30), Heilongjiang (~25% until Feb 5), Beijing (~15% until Feb 3), Shanghai (~20% until Jan 30), Yunnan (~75% until Jan 27), Hainan (~10% until Feb 5), Guizhou (~25% until Feb 1), Jilin (~30% until Feb 3). Some other provinces managed to decrease the growth rate exponentially during this period. As of Feb 1<sup>st</sup>, 15 provinces had reached the peak of the incidence curve, indicating the effectiveness of the extreme measures, and most provinces started to be in control of the epidemics.
- **Phase III (Feb 2 – Feb 14, 13 days): slow growth phase approaching the end of the outbreak.** In this period, all provinces continued to implement their strict measures, striving to bring the epidemics to an end. The growth rate of the number of confirmed cases declined exponentially with similar rates as in Phase II, pushing down the growth rate from 10% to 1%. In phase III, all provinces have passed the peak of the incidence curve, which allows us to

obtain precise scenarios for the dynamics of the end of the outbreak from the model fits (Figure 2). As of Feb 14, 23 out of 30 provinces have less than 10 new cases per day.

- **Phase IV (Feb 15 – 8 March): the end of the outbreak.** Starting Feb 15, the exponential decay of the growth rate at the aggregate level has switched to an even faster decay with parameter of 0.277 (Figure 1). As of Feb 17, one week after normal work being allowed to resume in most provinces, 22 provinces have a growth rate smaller than 1%. As of Feb 21, 28 provinces have achieved 5-day average growth rates smaller than 1%.

## **5. Analysis of the development of the epidemic and heterogenous provincial responses**

### **5.1 Quantification of the initial reactions and ramping up of control measures**

On Jan 19, Guangdong was the first province to report a confirmed infected patient outside Hubei. On Jan 20, 14 provinces reported their own first case. During Jan 21-23, another 14 provinces reported their first cases. If we determine the peak of the outbreak from the 5 days moving average of the incidence curve, then there are 15 provinces taking 7-11 days from their first case to their peak, 9 provinces taking 12-15 days, and 6 provinces taking more than 15 days. If we define the end of the outbreak as the day when the 5 days moving average of the growth rate becomes smaller than 1%, then 7 provinces spent 8-12 days from the peak to the end, 7 provinces spent 13-16 days, 13 provinces spent 17-20 days, and 2 provinces spent 21-22 days. For the six provinces that have the longest duration from the start of their outbreak to the peak (more than 15 days), it took 8-13 days for them to see the end of the outbreak (Figure 3). This means that these 6 provinces were able to control the local transmissions of the imported cases quite well, so that the secondary transmissions were limited. In contrast, 20 provinces took 28-31 days from the start to the end of the outbreak. Thus, those provinces that seem to have responded sluggishly during the early phase of the epidemics seem to have ramped up aggressively their countermeasures to achieve good results.

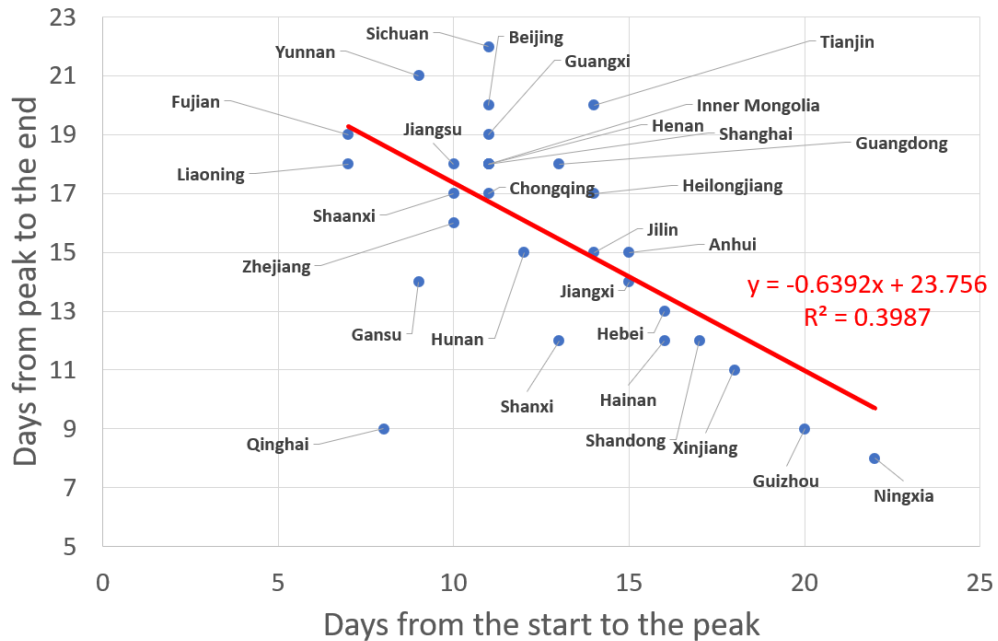


**Figure 3.** Inverse relationship found across the 29 Chinese provinces between the number of days from peak to the end and the duration from start to the peak of the epidemics. Here, the end of the outbreak is defined operationally as the day when the 5 days moving average of the growth rate becomes smaller than 1%.

## 5.2 Diagnostic of the efficiency of control measures from the exponential decay of the growth rate of infected cases

The 10 most infected provinces (Guangdong, Henan, Zhejiang, Hunan, Anhui, Jiangxi, Shandong, Jiangsu, Chongqing, Sichuan) have done quite well in controlling the transmission, as indicated by the fact that their daily growth rates follow well-defined exponential decays, with all of their  $R^2$  larger than 90%. This exponential decay continued for all ten provinces until the situation was completely under control during Feb 15-18, when the daily incidence was at near zero or a single-digit number. Eight out of these ten provinces have an exponential decay exponent of the growth rate ranging from 0.142 to 0.173, similar to what is observed at the national average level (0.157). Note that this exponential decay can be inferred from the generalized Richards model, as we noted in Eq (5) and (6) in Section 4.1.

## 5.3 Zhejiang and Henan exemplary developments

Zhejiang and Henan are the 2<sup>nd</sup> and 3<sup>rd</sup> most infected provinces but have the fastest decaying speed of the incidence growth rate (exponential decay exponent for Zhejiang: 0.223, Hunan: 0.186) among the most infected provinces. This is

consistent with the fast and strong control measures enforced by both provincial governments, which have been praised a lot on Chinese social network[38,39]. As one of the most active economies in China and one of the top provinces receiving travelers from Wuhan around the Lunar New Year[40], Zhejiang was the first province launching the top-level public health emergency on Jan 23<sup>rd</sup>, and implemented strong immediate measures, such as closing off all villages in some cities. The fitted curves from the GRM and logistic growth models indicate a peak of the incidence curve on Jan 31, which is the earliest time among top infected provinces. Similarly, Henan Province, as the neighbor province of Hubei and one of the most populated provinces in China, announced the suspension of passenger bus to and from Wuhan at the end of Dec 2019. In early Jan 2020, Henan implemented a series of actions including suspending poultry trading, setting up return spots at the village entrances for people from Hubei, listing designated hospitals for COVID-19 starting as early as Jan 17, and so on[39]. These actions were the first to be implemented among all provinces.

#### **5.4 Heterogeneity of the development of the epidemic and responses across various provinces**

Less infected provinces exhibit a larger variance in the decaying process of the growth rate. However, we also see good examples like Shanghai, Fujian and Shanxi, which were able to reduce the growth rate consistently with a low variance. These provinces benefited from experience obtained in the fight against the 2003 SARS outbreak or enjoy richer local medical resources[41]. This enabled the government to identify as many infected/suspected cases as possible in order to contain continuously the local transmissions. Bad examples include Heilongjiang, Jilin, Tianjin, Gansu, which is consistent with the analysis of [41].

Most provinces have a small parameter of  $p$  in the GRM (see Equation (4)) and an exponent  $\alpha$  large than 1, indicating that China was successful in containing the outbreak as sub-exponential growing process ( $p < 1$ ), with a faster than logistic decay ( $\alpha > 1$ ) in most provinces, except Guangdong, Zhejiang, Jiangxi, Sichuan, Heilongjiang, Fujian, Yunnan and Gansu. However, these exceptional provinces are due various reasons, which may not necessarily be the ineffective measures. The large  $p$  and small  $\alpha$  in Guangdong and Zhejiang are likely due to their high population densities and highly mobile populations in mega-cities, which are

factors known to largely contribute to the fast transmission of viruses. Jiangxi, Sichuan, Fujian, Yunnan and Gansu all had a fast growth phase before Feb 1<sup>st</sup>, but were successful in controlling the subsequent development of the epidemics. The fast growth phase in Heilongjiang lasted a bit longer than the abovementioned provinces, due to the occurrence of numerous local transmissions. Heilongjiang is the northernmost province in China, so it is far from Hubei and does not have a large number of migrating people from Hubei. However, compared with other provinces, it has a high statistic of both the confirmed cases and the case fatality rate (2.7% as of March 10), which has been criticized a lot by the Chinese social network.

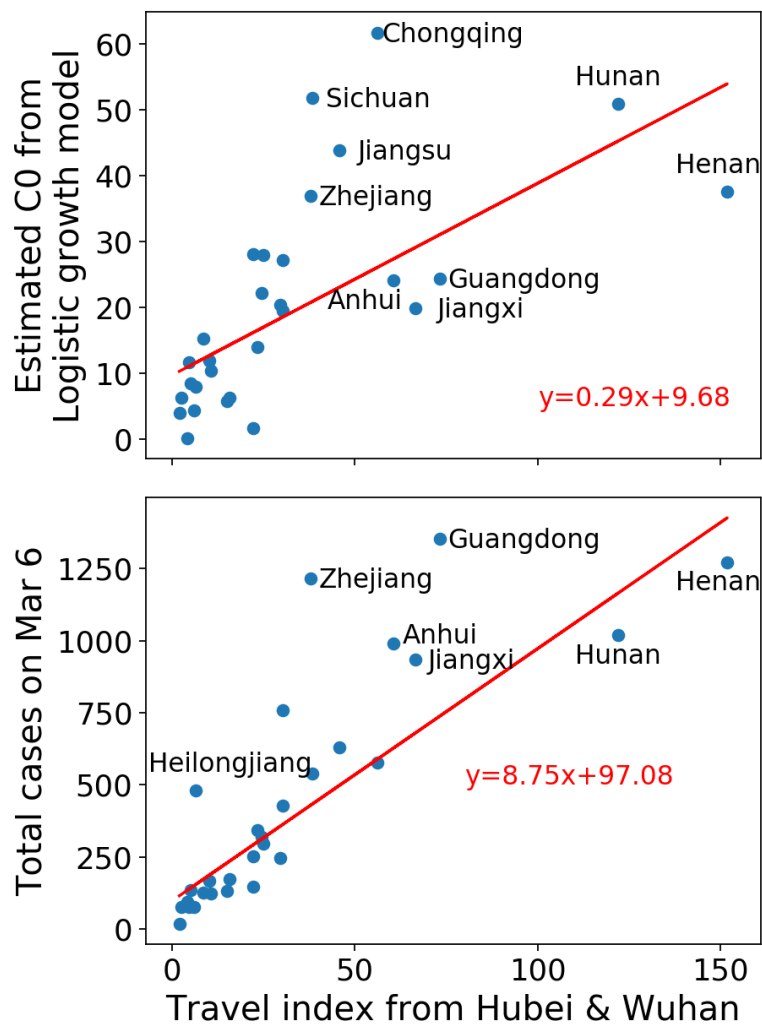


**Figure 4.** Upper panel: estimated  $C_0$  for the logistic growth model versus travel index from Hubei & Wuhan. Lower panel: total confirmed cases versus travel index from Hubei & Wuhan. The Pearson correlation between  $C_0$  and the migration index is 0.65 ( $p < 10^{-3}$ ), and the correlation between the cumulative number of confirmed cases and the migration index is 0.82 ( $p < 10^{-4}$ ).

## 5.5 Initial and total confirmed numbers of infected cases correlated with travel index

The initial value  $C_0$  of the logistic equation could be used as an indicator of the early number of cases, reflecting the level of early contamination from Hubei province as the epicenter of the outbreak. To support this proposition, the upper panel of Figure 4 plots the estimated  $C_0$  as a function of the migration index from Hubei & Wuhan to each province. The migration index is calculated as equal to 25% of the population migrating from Hubei (excluding Wuhan) plus 75% of the population migrating from Wuhan, given that Wuhan was the epicenter and the risks from the Hubei region excluding Wuhan are lower. One can observe a clear positive correlation between the estimated  $C_0$  and the migration index. The lower panel of Figure 4 shows an even stronger correlation between the total number of cases recorded on March 6<sup>st</sup> and the travel index, expressing that a strong start of the epidemics predicts a larger number of cases, which is augmented by infections resulting from migrations out of the epidemic epicenter.

## 6. Analysis and scenario predictions of the epidemic for various countries

In this section, we use the four models (Eq. 1-4) and the resulting three scenarios we specified in Section 3 to analyze the status of different countries and project future scenarios.

As of April 24, Europe has cumulatively 1.26 million confirmed cases with a growth rate of 2-3% per day, gradually decreased from more than 10% a month ago. The United States has cumulatively 870 thousand confirmed cases with a growth rate of 3-5% per day, decreased from more than 10% twenty days ago. The fitting results of the four models to the data from Europe and the US are presented in Figures 5 and 6. We argue that both Europe (as a whole) and the US have passed the inflection point and are in an after-peak trajectory of the outbreak. At this stage, the daily incidence curve of both Europe and the US have largely departed from a (sub-)exponential growth path with the Generalized Growth Model (GGM) having the lowest  $R^2$  among the four models, while the Generalized Richards Model (GRM) obtains the highest  $R^2$ . This complies with our understanding that the GRM can better describe the outbreak in an after-peak stage, as it can capture richer

dynamics of the epidemic, in the form of the slow decay of the after-peak trajectory in the case of Europe and the US. Mathematically, this is associated with the small estimated parameter  $\alpha$  of GRM in the two regions (Europe: 0.21 with 80% confidence interval of [0.18, 0.78], US: 0.27 with 80% confidence interval of [0.14, 1.1]). Note that this is contrary to the results of the majority of provinces in China in the after-peak stage, possibly due to the heterogenous outbreak stages and containment measures within Europe and the US. The extreme lockdown and containment measures in China were implemented strictly through the whole period of the outbreak with centralized management, contributing to the fast decay of the outbreak in the after-peak stage. However, the western countries have utilized very different containment measures, leading to different results among regions and a slow decay as a whole. In the medium scenario, we expect Europe to have 1.83 (80% prediction interval: [1.7, 1.97]) million confirmed cases in the end, corresponding to 2452 ([2278, 2639]) confirmed cases per million population. Regarding US, it is estimated to have 1.26 (80% prediction interval: [1.12, 1.39]) million confirmed cases in the end, corresponding to 3851 ([3423, 4249]) confirmed cases per million population.

In Table 2, we report the latest confirmed cases per million population and the estimated outbreak progress in the positive and medium scenarios for various countries. The outbreak progress is defined as the latest confirmed cases divided by the estimated final total confirmed case, either in the positive or the medium scenario. In Figure 7, we present the distribution of the estimated final total confirmed cases per million population obtained by aggregating the positive and medium scenarios. The figures showing fitting results for each country like Figure 5 and 6 can be found in the supplementary material. The most matured group of countries include Austria, Switzerland, Germany, France, Spain, Italy, Portugal and Ireland, which have strong signs that inflection points have been passed and have an outbreak progress larger than 80% in the medium scenario. The outbreak progress in Austria reaches 100%, indicating the end of the outbreak is in sight as measured by new confirmed cases. These countries include the earliest hotspots of the outbreak in Italy and Spain, followed by Austria, Switzerland, Germany, and France. Among them, Austria and Switzerland are the two most mature countries, and have been the first European countries to publish their timetable for progressively lifting the lockdown measures [42,43].

The next group of countries include Belgium, Turkey, Netherlands, and the UK, which are less matured with outbreak progress in the range 60-80% in the medium scenario. They have developed signs of passing their inflection points, but are less matured and may reverse to their previous exponential growth. All of these four countries and the 8 matured countries mentioned above have their distributions of final confirmed cases converged, indicating reliability of the future projected scenarios.

The least mature group of countries are Japan, Russia, Sweden and Brazil, which have just flattened the curve (Russia and Japan) or still in the exponential growth stage (Sweden and Brazil), indicating highly uncertain future projections, as shown by their non-converged or highly dispersed ensemble distributions of final confirmed cases (Figure 7).

Trajectories from Iran and South Korea have largely deviated from a typical logistic type growth (S-curve), and can't be properly described by our models. Iran has a long plateau period and we highly suspect the data reliability from Iran, especially in the early stage. The first wave of the outbreak in South Korea starting mid-Feb can be well described by a Logistic type model, however there is a long tail of the daily incidence curve after the major outbreak of the first wave was under control in mid-March. We expect Europe and US will also have a long tail after the major outbreak is under control, because it might be difficult to eradicate this highly infectious virus in the absence of early and extreme measures. However, it is not realistic to continue stopping all social and economic activities when there is no large-scale epidemics.

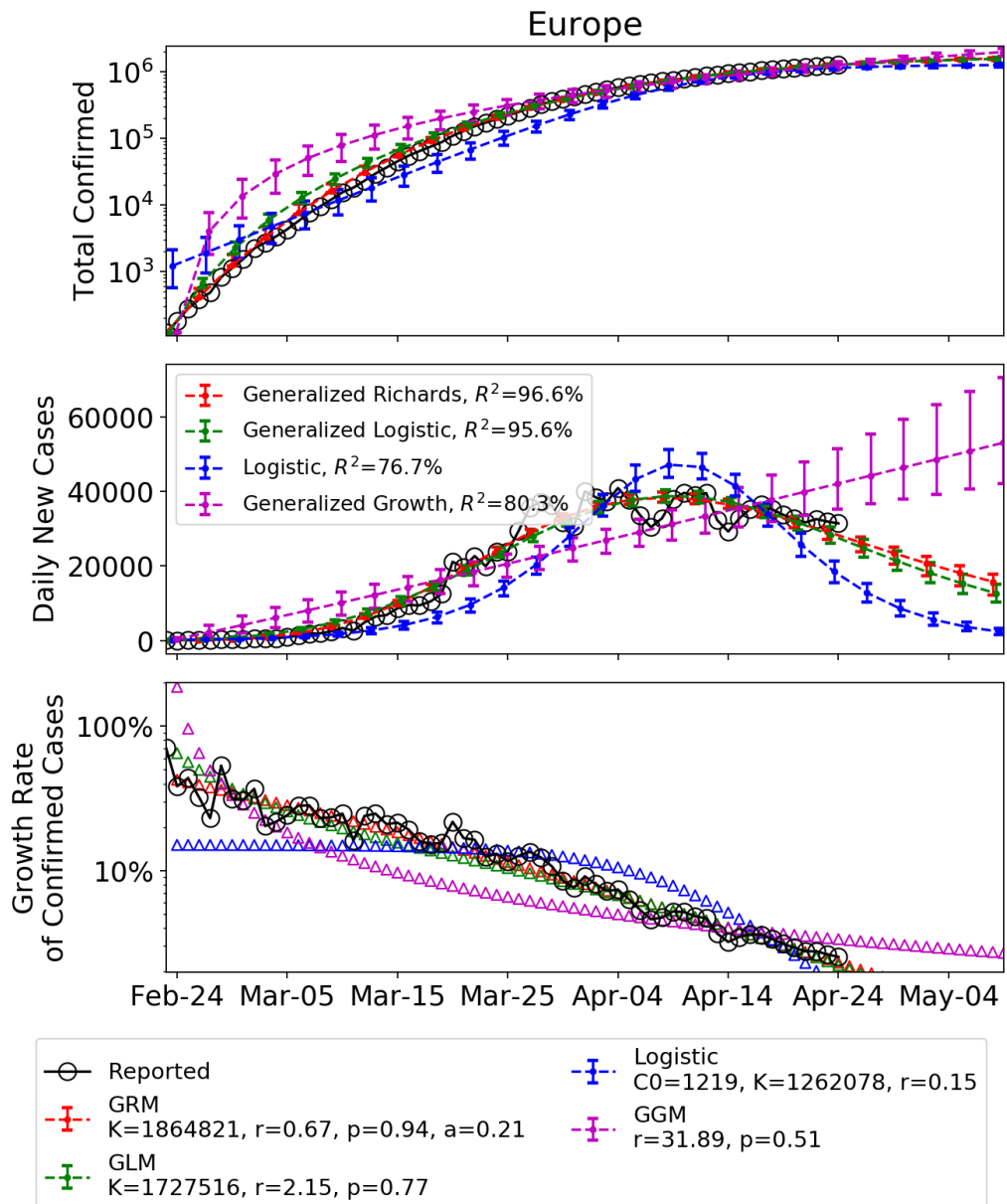


**Figure 5.** The total number of confirmed cases, daily confirmed cases and the daily growth rate of the Europe are plotted in the upper, middle and lower panel respectively. The empirical data is marked by the empty circles. The blue, red, purple and green lines in the upper, middle and lower left panels show the fits with the Logistic Growth Model, Generalized Richards Model (GRM), Generalized Growth Model (GGM) and Generalized Logistic Model (GLM) respectively. The error bars indicate 80% prediction intervals. Data is plotted every 3 days.

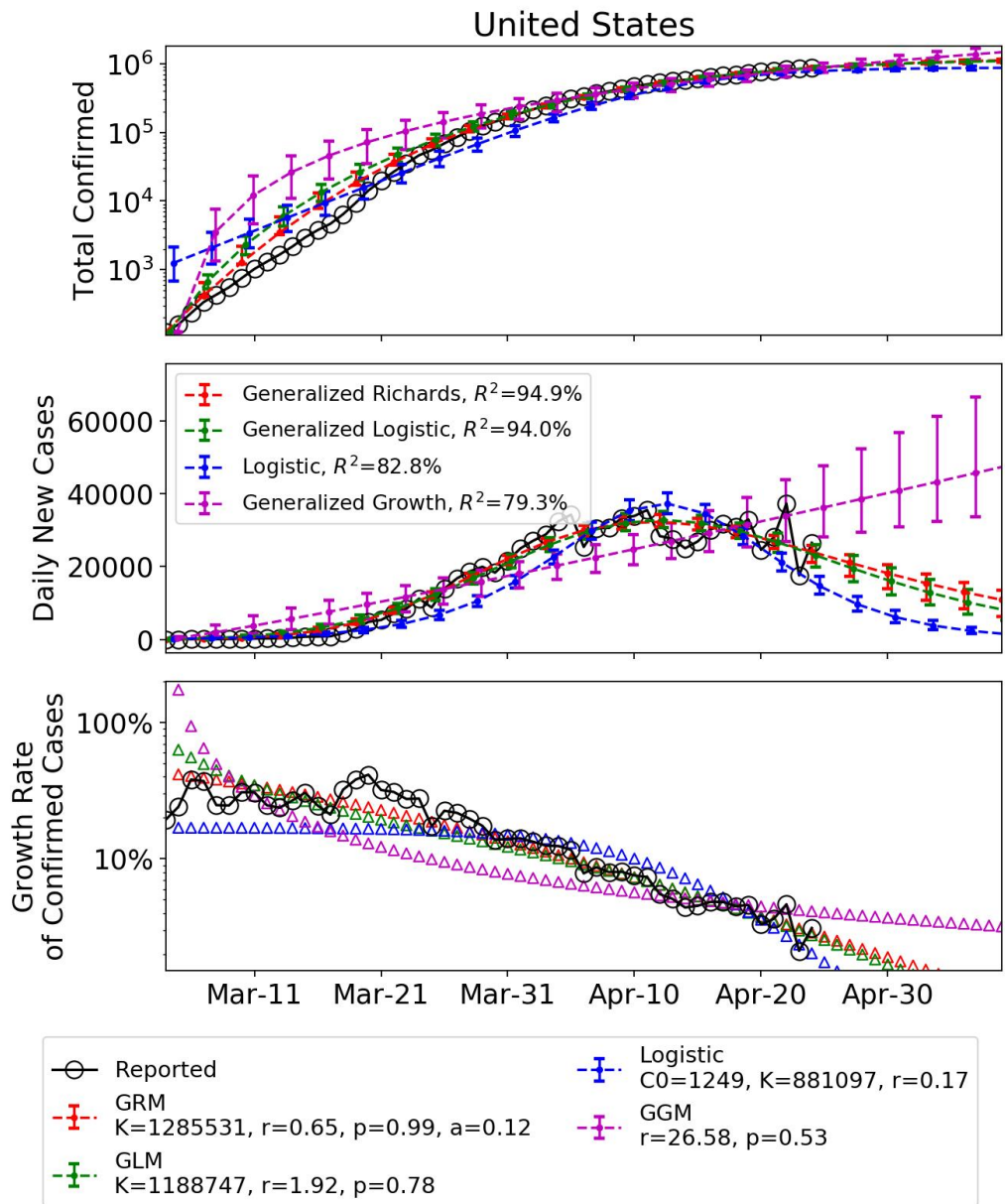


**Figure 6.** The total number of confirmed cases, daily confirmed cases and the daily growth rate of the US are plotted in the upper, middle and lower panel respectively. The empirical data is marked by the empty circles. The blue, red, purple and green lines in the upper, middle and lower left panels show the fits with the Logistic Growth Model, Generalized Richards Model (GRM), Generalized Growth Model (GGM) and Generalized Logistic Model (GLM) respectively. The error bars indicate 80% prediction intervals. Data is plotted every 3 days.

**Table 2.** Current confirmed cases per million population and estimated outbreak progress in positive and medium scenarios (April 24 confirmed cases divided by the estimated total final confirmed cases in positive and medium scenario). The ranking is in terms of outbreak progress in medium scenario (fourth column from left). Numbers in brackets are 80% confidence intervals. As positive scenarios predict a smaller final number of total infected cases, the outbreak progress is thus larger in the positive scenario. Note that the estimated final confirmed numbers tend to

underestimate the final results, thus the estimated outbreak progress serves both as a lower bound for future developments and as a guide of the dynamics of the evolution of the epidemics. The number of tests per million population and confirmed cases per test are presented in the last two columns based on the data aggregated by Wikipedia[44].

	Confirmed per Million Population (Apr-24)	Outbreak Progress in <b>Positive</b> Scenario	Outbreak Progress in <b>Medium</b> Scenario	Tests per Million Population (update date in brackets)	Confirmed Cases per Test (update date in brackets)
Austria	1694	100.0% (93.5%, 100%)	99.9% (94.8%, 100%)	23890 (Apr 24)	7.0% (Apr 24)
Switzerland	3336	93.8% (88.3%, 99.1%)	93.0% (88.6%, 97.5%)	26948 (Apr 22)	12.1% (Apr 22)
Germany	1813	92.5% (87.9%, 97.4%)	91.5% (87.5%, 95.0%)	24927 (Apr 21)	6.9% (Apr 21)
France	1803	90.7% (83.4%, 99.3%)	90.2% (81.8%, 98.4%)	6823 (Apr 19)	24.5% (Apr 19)
Spain	4559	89.3% (83.1%, 95.7%)	87.3% (82.8%, 91.6%)	19905 (Apr 13)	17.8% (Apr 13)
Italy	3144	86.4% (82.2%, 91.1%)	84.6% (81.3%, 88.3%)	27210 (Apr 24)	11.6% (Apr 24)
Portugal	2174	81.8% (73.3%, 89.4%)	81.3% (71.9%, 90.8%)	22953 (Apr 23)	7.3% (Apr 23)
Ireland	3628	81.8% (71.1%, 89.7%)	80.3% (71.3%, 89.0%)	23433 (Apr 20)	13.7% (Apr 20)
Belgium	3747	76.2% (67.6%, 84.3%)	72.9% (63.3%, 84.6%)	14059 (Apr 20)	23.8% (Apr 20)
Turkey	1237	74.1% (62.1%, 82.8%)	70.9% (65.3%, 75.3%)	9984 (Apr 24)	12.3% (Apr 24)
Netherlands	2074	74.4% (69.2%, 78.9%)	69.6% (63.9%, 76.6%)	9470 (Apr 20)	19.8% (Apr 20)
United States	2657	72.9% (65.7%, 80.4%)	69.1% (62.4%, 77.6%)	14892 (Apr 24)	17.8% (Apr 24)
Europe	1691	73.5% (68.5%, 77.7%)	69.0% (64.1%, 74.1%)	NA	NA
United Kingdom	2077	72.3% (66.6%, 78.4%)	68.6% (60.5%, 76.0%)	9061 (Apr 24)	22.6% (Apr 24)
Japan	98	84.2% (79.0%, 88.7%)	59.1% (46.9%, 65.5%)	1122 (Apr 24)	8.7% (Apr 24)
Russia	434	60.1% (53.3%, 66.5%)	53.5% (44.9%, 57.8%)	17391 (Apr 23)	2.3% (Apr 23)
Sweden	1645	48.0% (19.5%, 86.2%)	43.9% (26.3%, 58.8%)	9150 (Apr 21)	15.6% (Apr 21)
Brazil	236	28.3% (7.7%, 88.3%)	12.3% (0.0%, 45.5%)	2496 (Apr 20)	7.4% (Apr 20)
Iran	1064	Not reliable	Not reliable	4397 (Apr 21)	22.8% (Apr 21)
South Korea	207	Not reliable	Not reliable	11293 (Apr 23)	1.8% (Apr 23)

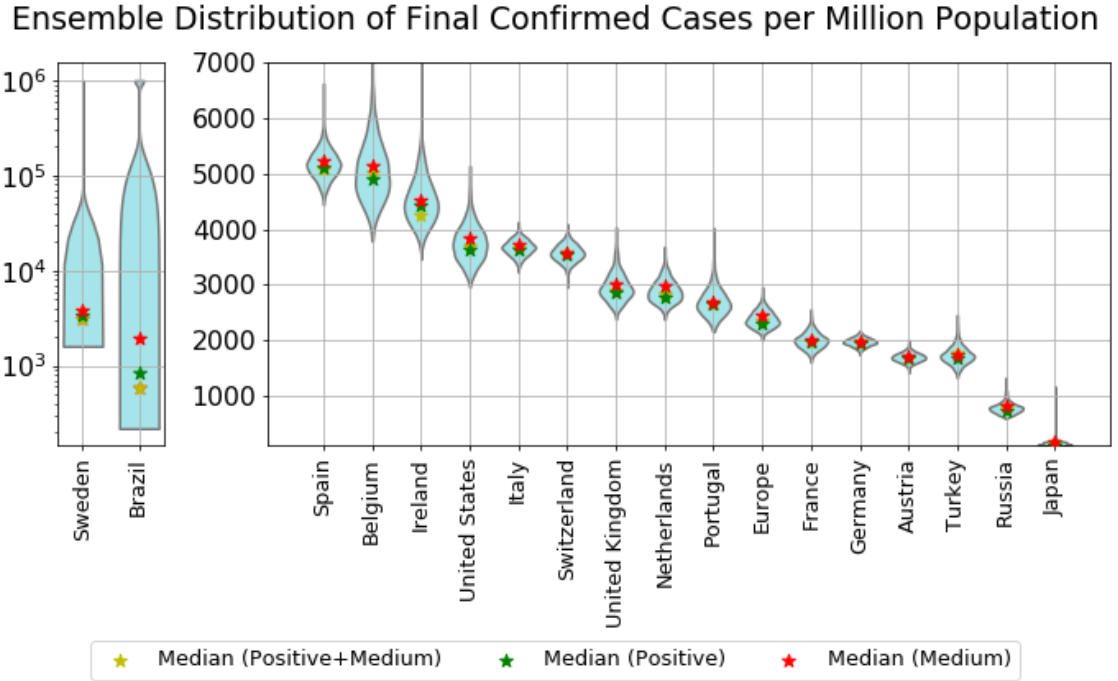


**Figure 7.** Violin plot of the distributions of the final total number of confirmed cases per million derived by combining the distributions of the positive and medium scenarios. The left side of each violin in cyan is today's distribution, while the right side of each violin in grey is yesterday's distribution. The model setup in the negative scenario does not incorporate a maximum saturation number and thus cannot be used. The yellow star indicates the median prediction for the combined distribution, while the green and red stars indicate the median of the positive and of the medium scenarios respectively. Note that, where we have  $>1$  million infections or deaths per 1 million of population, the results are deemed to be unreliable (Table 2 & 3).

## 7. Discussion on the limitation of the method

In this paper, we only apply the models to the number of confirmed cases, which is largely subject to a number of extraneous variations among countries such as case definition, testing capacity, testing protocol, reporting system, etc. It is important to note that there is a significant limitation by using this statistic to estimate the true situation of the outbreak in a country, and we lay out four major variables here:

- **Case definition.** Different countries employ different definitions of a confirmed COVID-19 case, and the definition also changes over the time. For example, China's national health commission issued seven versions of a case definition for COVID-19 between 15 January and 3 March, and a recent study found each of the first four changes increased the proportion of cases detected and counted by factors between 2.8 and 7.1 [45].

- **Testing capacity.** The number of confirmed cases is usually determined by testing, which is biased towards severe cases in some countries like France. In contrast, the testing is aimed at a larger group in some other countries implementing massive testing programs, such as South Korea and Iceland. Based on antibody tests performed on the general population, several reports show that the actual number of infected people is much larger than the reported value [46,47].
- **Testing protocol.** The testing protocols and accuracy may also have a large impact on the results. Depending on the testing protocols used, in some instances, false positive results have been obtained. In other words, someone without the disease tested positive, probably because they were infected with some other coronavirus. There have been several reports raising this issue [48]. On the other hand, false negative results may also exist and seem to be more prevalent than false positives.
- **Reporting system and time.** Data also relies on the efficiency of the reporting system. Tests are conducted sequentially over time and the reported data may be adjusted afterwards. They do not represent a snapshot of a day in time. For instance, the Netherlands National Institute for Public Health and the Environment clearly states that some of the positive results are only reported one or a few days later and there might be corrections for the past data, so the numbers from a few days ago are sometimes adjusted[48].

Therefore, the real number of cases in the population is likely to be many multiples higher than those computed from confirmed tests and the number of confirmed cases can only reflect the real situation of the outbreak to some degree. This may also partly explain that the Logistic model fails to capture the growth dynamics at the early stage in most provinces in China, as showed in Section 5, likely due to the potential underreporting at the beginning.

The Logistic type of models are relatively accurate in short-term predictions, while they tend to underestimate the final confirmed numbers in the long term, which has a higher uncertainty. Thus the three Logistic type models could only provide a lower bound for the future scenarios. As more data becomes available, we anticipate a more accurate picture of the final numbers, as showed by the

converged ensemble distributions in Austria and Switzerland with small variance. As a last remark, even if the true number of cases is a multiple of the reported number of confirmed cases, as long as the multiple does not vary too much for a given country, our analysis remains pertinent to ascertain the outbreak progress and nature of the epidemic dynamics.

## 8. Conclusion

In this paper, we calibrated the logistic growth model, the generalized logistic growth model, the generalized growth model and the generalized Richards model to the reported number of confirmed cases in the Covid-19 epidemics from Jan. 19 to March 10 for the whole of China and for the 29 provinces in China. This has allowed us to draw some lessons useful to interpret the results of a similar modeling exercise performed on other countries, which are in the middle of an outbreak. Our analysis dissects the development of the epidemics in China and the impact of the drastic control measures both at the aggregate level and within each province. We documented four phases: I- early stage outbreak (Jan 19 – Jan 24, 6 days), II- fast growth phase approaching the peak of the incidence curve (Jan 25 – Feb 1, 8 days), III- slow growth phase approaching the end of the outbreak (Feb 2 – Feb 14, 13 days) and IV- the end of the outbreak (Feb 15 – 8 March). We quantified the initial reactions and ramping up of control measures on the dynamics of the epidemics and unearthed an inverse relationship between the number of days from peak to the quasi-end and the duration from start to the peak of the epidemic among the 29 analyzed Chinese provinces. We identified the dynamic signatures of the exemplary developments in Zhejiang and Henan provinces and the heterogeneity of the development of the epidemic and responses across various other provinces. We found a strong correlation between the initial and total confirmed numbers of infected cases and travel index quantifying the mobility between provinces.

For countries that are in the middle of the outbreak, we constructed three future scenarios to make future projections. We identified that Europe and US have passed the inflection point and entered into an after-peak trajectory. We found that this stage might be longer than what a classical Logistic model predicts, in contrast to most provinces in China where the after-peak trajectory is much faster than the Logistic decay, possibly due to the strict containment measures in China. We expect Europe to have 1.83 (80% prediction interval: [1.7, 1.97]) million confirmed cases

in the end, corresponding to 2452 ([2278, 2639]) confirmed cases per million population, and US to have 1.26 (80% prediction interval: [1.12, 1.39]) million final confirmed cases, corresponding to 3851 ([3423, 4249]) per million population. We found that 8 countries (Austria, Switzerland, Germany, France, Spain, Italy, Portugal and Ireland) have entered into the final stage of the epidemic, which might last until end of May, while Japan, Russia, Sweden and Brazil are at the least mature stage.

## **Declarations**

### **Funding**

No funding information is applicable.

### **Conflicts of interest/Competing interests**

The authors declare that they have no competing interests

### **Availability of data and material**

The datasets generated and analysed during the current study are available in the Github repository, <https://github.com/kezida/covid-19-logistic-paper>

### **Code availability**

Code is available upon request.

### **Authors' contributions**

KW and DS designed the research. KW and QW performed the data analysis. All authors wrote, read and approved the final manuscript.

## Reference

1. Dye, C., Gay, N.: Modeling the SARS epidemic. *Science* **300**(5627), 1884-1885 (2003). doi:10.1126/science.1086925
2. Laguzet, L., Turinici, G.: Individual vaccination as Nash equilibrium in a SIR model with application to the 2009–2010 influenza A (H1N1) epidemic in France. *Bulletin of Mathematical Biology* **77**(10), 1955-1984 (2015). doi:10.1007/s11538-015-0111-7
3. Zhao, Z., Calderón, J., Xu, C., Zhao, G., Fenn, D., Sornette, D., Crane, R., Hui, P.M., Johnson, N.F.: Effect of social group dynamics on contagion. *Physical Review E* **81**(5), 056107 (2010). doi:10.1103/PhysRevE.81.056107
4. Lekone, P.E., Finkenstädt, B.F.: Statistical inference in a stochastic epidemic SEIR model with control intervention: Ebola as a case study. *Biometrics* **62**(4), 1170-1177 (2006). doi:10.1111/j.1541-0420.2006.00609.x
5. Smieszek, T., Balmer, M., Hattendorf, J., Axhausen, K.W., Zinsstag, J., Scholz, R.W.: Reconstructing the 2003/2004 H3N2 influenza epidemic in Switzerland with a spatially explicit, individual-based model. *BMC Infectious Diseases* **11**(1), 115 (2011). doi:10.1186/1471-2334-11-115
6. Chang, S.L., Piraveenan, M., Pattison, P., Prokopenko, M.: Game theoretic modelling of infectious disease dynamics and intervention methods: a review. *Journal of Biological Dynamics* **14**(1), 57-89 (2020). doi:10.1080/17513758.2020.1720322
7. Chang, S.L., Harding, N., Zachreson, C., Cliff, O.M., Prokopenko, M.: Modelling transmission and control of the COVID-19 pandemic in Australia. *arXiv preprint arXiv:2003.10218* (2020).
8. Prem, K., Liu, Y., Russell, T.W., Kucharski, A.J., Eggo, R.M., Davies, N., Flasche, S., Clifford, S., Pearson, C.A.B., Munday, J.D., Abbott, S., Gibbs, H., Rosello, A., Quilty, B.J., Jombart, T., Sun, F., Diamond, C., Gimma, A., van Zandvoort, K., Funk, S., Jarvis, C.I., Edmunds, W.J., Bosse, N.I., Hellewell, J., Jit, M., Klepac, P.: The effect of control strategies to reduce social mixing on outcomes of the COVID-19 epidemic in Wuhan, China: a modelling study. *The Lancet Public Health* (2020). doi:[https://doi.org/10.1016/S2468-2667\(20\)30073-6](https://doi.org/10.1016/S2468-2667(20)30073-6)
9. Hou, C., Chen, J., Zhou, Y., Hua, L., Yuan, J., He, S., Guo, Y., Zhang, S., Jia, Q., Zhao, C., Zhang, J., Xu, G., Jia, E.: The effectiveness of quarantine of Wuhan city against the Corona Virus Disease 2019 (COVID-19): A well-mixed SEIR model analysis. *Journal of Medical Virology* **n/a**(n/a). doi:10.1002/jmv.25827
10. Boldog, P., Tekeli, T., Vizi, Z., Dénes, A., Bartha, F.A., Röst, G.: Risk assessment of novel coronavirus COVID-19 outbreaks outside China. *Journal of clinical medicine* **9**(2), 571 (2020). doi:10.3390/jcm9020571
11. Rocklöv, J., Sjödin, H., Wilder-Smith, A.: COVID-19 outbreak on the Diamond Princess cruise ship: estimating the epidemic potential and effectiveness of public health countermeasures. *Journal of Travel Medicine* (2020). doi:10.1093/jtm/taaa030
12. Ferguson, N., Laydon, D., Nedjati Gilani, G., Imai, N., Ainslie, K., Baguelin, M., Bhatia, S., Boonyasiri, A., Cucunuba Perez, Z., Cuomo-Dannenburg, G., Dighe, A., Dorigatti, I., Fu, H., Gaythorpe, K., Green, W., Hamlet, A., Hinsley, W., Okell, L.C., van Elsland, S., Thompson, H.,

Verity, R., Volz, E., Wang, H., Wang, Y., Walker, P.G., Walters, C., Winskill, P., Whittaker, C., Donnelly, C.A., Riley, S., Ghani, A.C.: Report 9: Impact of non-pharmaceutical interventions (NPIs) to reduce COVID19 mortality and healthcare demand. (2020). doi:10.25561/77482

13. Sornette, D.: Predictability of catastrophic events: Material rupture, earthquakes, turbulence, financial crashes, and human birth. *Proceedings of the National Academy of Sciences* **99**(suppl 1), 2522-2529 (2002). doi:10.1073/pnas.022581999

14. Sornette, D.: Critical phenomena in natural sciences: chaos, fractals, selforganization and disorder: concepts and tools. Springer Science & Business Media, (2006)

15. Israeli, N., Goldenfeld, N.: Computational irreducibility and the predictability of complex physical systems. *Physical review letters* **92**(7), 074105 (2004). doi:10.1103/PhysRevLett.92.074105

16. Chowell, G., Hincapie-Palacio, D., Ospina, J., Pell, B., Tariq, A., Dahal, S., Moghadas, S., Smirnova, A., Simonsen, L., Viboud, C.: Using Phenomenological Models to Characterize Transmissibility and Forecast Patterns and Final Burden of Zika Epidemics. *PLoS Currents* **8** (2016). doi:10.1371/currents.outbreaks.f14b2217c902f453d9320a43a35b9583

17. You, C., Deng, Y., Hu, W., Sun, J., Lin, Q., Zhou, F., Pang, C.H., Zhang, Y., Chen, Z., Zhou, X.-H.: Estimation of the time-varying reproduction number of COVID-19 outbreak in China. Available at SSRN 3539694 (2020). doi:10.2139/ssrn.3539694

18. Tuite, A.R., Fisman, D.N.: Reporting, Epidemic Growth, and Reproduction Numbers for the 2019 Novel Coronavirus (2019-nCoV) Epidemic. *Annals of Internal Medicine* **172**, 567-568 (2020). doi:10.7326/M20-0358

19. Zhao, S., Cao, P., Gao, D., Zhuang, Z., Chong, M.K., Cai, Y., Ran, J., Wang, K., Yang, L., He, D.: Epidemic growth and reproduction number for the novel coronavirus disease (COVID-19) outbreak on the Diamond Princess Cruise Ship from January 20 to February 19, 2020: a preliminary data-driven analysis. Available at SSRN 3543150 (2020). doi:10.2139/ssrn.3543150

20. Zhang, S., Diao, M., Yu, W., Pei, L., Lin, Z., Chen, D.: Estimation of the reproductive number of Novel Coronavirus (COVID-19) and the probable outbreak size on the Diamond Princess cruise ship: A data-driven analysis. *International Journal of Infectious Diseases* **93**, 201-204 (2020). doi:10.1016/j.ijid.2020.02.033

21. Remuzzi, A., Remuzzi, G.: COVID-19 and Italy: what next? *The Lancet* **395**(10231), 1225-1228 (2020). doi:10.1016/S0140-6736(20)30627-9

22. Maier, B.F., Brockmann, D.: Effective containment explains sub-exponential growth in confirmed cases of recent COVID-19 outbreak in Mainland China. *arXiv preprint arXiv:2002.07572* (2020).

23. Muniz-Rodriguez, K., Chowell, G., Cheung, C.-H., Jia, D., Lai, P.-Y., Lee, Y., Liu, M., Ofori, S.K., Roosa, K.M., Simonsen, L., Viboud, C.G., Fung, I.C.-H.: Epidemic doubling time of the COVID-19 epidemic by Chinese province. *medRxiv* (2020). doi:10.1101/2020.02.05.20020750

24. Zhang, J., Litvinova, M., Wang, W., Wang, Y., Deng, X., Chen, X., Li, M., Zheng, W., Yi, L., Chen, X., Wu, Q., Liang, Y., Wang, X., Yang, J., Sun, K., Jr, I.M.L., Halloran, M.E., Wu, P., Cowling, B.J., Yu, H.: Evolving epidemiology of novel coronavirus diseases 2019 and possible

interruption of local transmission outside Hubei Province in China: a descriptive and modeling study. *medRxiv*, 1-9 (2020). doi:10.1101/2020.02.21.20026328

25. Roosa, K., Lee, Y., Luo, R., Kirpich, A., Rothenberg, R., Hyman, J.M., Yan, P., Chowell, G.: Real-time forecasts of the 2019-nCoV epidemic in China from February 5th to February 24th, 2020. *Infectious Disease Modelling* **5**, 256-263 (2020). doi:10.1016/j.idm.2020.02.002

26. Roosa, K., Lee, Y., Luo, R., Kirpich, A., Rothenberg, R., Hyman, J.M., Yan, P., Chowell, G.: Short-term Forecasts of the COVID-19 Epidemic in Guangdong and Zhejiang, China: February 13–23, 2020. *Journal of Clinical Medicine* **9**(2), 596-596 (2020). doi:10.3390/jcm9020596

27. Chowell, G.: Fitting dynamic models to epidemic outbreaks with quantified uncertainty: A primer for parameter uncertainty, identifiability, and forecasts. *Infectious Disease Modelling* **2**(3), 379-398 (2017). doi:10.1016/j.idm.2017.08.001

28. Viboud, C., Simonsen, L., Chowell, G.: A generalized-growth model to characterize the early ascending phase of infectious disease outbreaks. *Epidemics* **15**, 27-37 (2016). doi:10.1016/j.epidem.2016.01.002

29. Chowell, G., Tariq, A., Hyman, J.M.: A novel sub-epidemic modeling framework for short-term forecasting epidemic waves. *BMC Medicine* **17**(1), 1-18 (2019). doi:10.1186/s12916-019-1406-6

30. Chowell, G., Luo, R., Sun, K., Roosa, K., Tariq, A., Viboud, C.: Real-time forecasting of epidemic trajectories using computational dynamic ensembles. *Epidemics* **30**(November 2019), 100379-100379 (2020). doi:10.1016/j.epidem.2019.100379

31. Beaubien, J.: China Enters The Next Phase of Its COVID-19 Outbreak: Suppression. <https://www.npr.org/sections/goatsandsoda/2020/04/03/826140766/china-enters-the-next-phase-of-its-covid-19-outbreak-suppression> (2020). Accessed Apr 24 2020

32. European Centre for Disease Prevention and Control (ECDC): Situation update worldwide. <https://www.ecdc.europa.eu/en/geographical-distribution-2019-ncov-cases> (2020). Accessed Apr 24 2020

33. Ma, J., Dushoff, J., Bolker, B.M., Earn, D.J.: Estimating initial epidemic growth rates. *Bulletin of mathematical biology* **76**(1), 245-260 (2014). doi:10.1007/s11538-013-9918-2

34. Kermack, W.O., McKendrick, A.G.: A contribution to the mathematical theory of epidemics. *Proceedings of the royal society of london. Series A, Containing papers of a mathematical and physical character* **115**(772), 700-721 (1927). doi:10.1098/rspa.1927.0118

35. Richards, F.J.: A flexible growth function for empirical use. *Journal of Experimental Botany* **10**(2), 290-301 (1959). doi:10.1093/jxb/10.2.290

36. Neher, D.A., Campbell, C.L.: Underestimation of disease progress rates with the logistic, monomolecular, and gompertz models when maximum disease intensity is less than 100 percent. *Phytopathology* **82**(8), 811-814 (1992).

37. Pell, B., Kuang, Y., Viboud, C., Chowell, G.: Using phenomenological models for forecasting the 2015 Ebola challenge. *Epidemics* **22**, 62-70 (2018).

38. Tian, Y.: The tough time through the Chinese New Year (in Chinese: 既过年关，也过难关). [https://web.archive.org/web/20200125183422/http://www.xinhuanet.com/politics/2020-01/25/c\\_1125501347.htm](https://web.archive.org/web/20200125183422/http://www.xinhuanet.com/politics/2020-01/25/c_1125501347.htm) (2020). Accessed Jan 25 2020

39. He, X.: How strong is Henan in preventing and controlling COVID-19? (in Chinese: 防控肺炎病毒, "硬核"河南究竟有多硬核?). <http://www.nbd.com.cn/articles/2020-01-25/1402907.html> (2020). Accessed Jan 25 2020

40. Lai, S., Bogoch, I.I., Watts, A., Khan, K., Li, Z., Tatem, A.: Preliminary risk analysis of 2019 novel coronavirus spread within and beyond China. <https://www.pentapostagma.gr/sites/default/files/2020-02/worldpop-coronavirus-spread-risk-analysis-v1-25jan.pdf> (2020). Accessed Feb 25 2020

41. Ying, S., Li, F., Geng, X., Li, Z., Du, X., Chen, H., Chen, S., Zhang, M., Shao, Z., Wu, Y., Syeda, M.Z., Yan, F., Che, L., Zhang, B., Lou, J., Wang, S., Chen, Z., Li, W., Shen, Y., Chen, Z., Shen, H.: Spread and control of COVID-19 in China and their associations with population movement, public health emergency measures, and medical resources. medRxiv, 2020.2002.2024.20027623 (2020). doi:10.1101/2020.02.24.20027623

42. Swiss Federal Office of Public Health FOPH: Federal Council to gradually ease measures against the new coronavirus. <https://www.admin.ch/gov/en/start/documentation/media-releases.msg-id-78818.html> (2020). Accessed Apr 23 2020

43. Connolly, K.: Austria reopens small shops and parks as coronavirus lockdown is relaxed. <https://www.theguardian.com/world/2020/apr/14/austria-reopens-small-shops-and-parks-as-coronavirus-lockdown-is-relaxed> (2020). Accessed 2020 April 23

44. Wikipedia: COVID-19 testing statistics by country. [https://en.wikipedia.org/wiki/COVID-19\\_testing#Virus\\_testing\\_statistics\\_by\\_country](https://en.wikipedia.org/wiki/COVID-19_testing#Virus_testing_statistics_by_country) (2020). Accessed Apr 25 2020

45. Tsang, T.K., Wu, P., Lin, Y., Lau, E.H., Leung, G.M., Cowling, B.J.: Effect of changing case definitions for COVID-19 on the epidemic curve and transmission parameters in mainland China: a modelling study. The Lancet Public Health (2020). doi:10.1016/S2468-2667(20)30089-X

46. Bendavid, E., Mulaney, B., Sood, N., Shah, S., Ling, E., Bromley-Dulfano, R., Lai, C., Weissberg, Z., Saavedra, R., Tedrow, J., Tversky, D., Bogan, A., Kupiec, T., Eichner, D., Gupta, R., Ioannidis, J., Bhattacharya, J.: COVID-19 Antibody Seroprevalence in Santa Clara County, California. medRxiv, 2020.2004.2014.20062463 (2020). doi:10.1101/2020.04.14.20062463

47. Streeck, H., Hartmann, G., Exner, M., Schmid, M.: Preliminary results and conclusions of the COVID-19 case cluster study (Gangelt municipality) (in Germany: Vorläufiges Ergebnis und Schlussfolgerungen der COVID-19 Case-ClusterStudy (Gemeinde Gangelt)). [https://www.land.nrw/sites/default/files/asset/document/zwischenergebnis\\_covid19\\_case\\_study\\_gangelt\\_0.pdf](https://www.land.nrw/sites/default/files/asset/document/zwischenergebnis_covid19_case_study_gangelt_0.pdf) (2020). Accessed 2020 Apr 23

48. Environment, T.N.N.I.f.P.H.a.t.: Development of COVID-19 in graphs. <https://www.rivm.nl/coronavirus-covid-19/grafieken> (2020). Accessed 2020 Apr 23